Geometric model-based joint angle selection criterion for force parameter identification & Decoupling control method of position and posture in shaft-hole assembly

Junhe Wang, Yong Jiang*, Song Lin, Fanxu Kong

***Abstract*—Robotic vision servo technology has been developed to control a robotic arm to a specified position with the guidance of a vision sensor. However, for tasks that require high precision control, guidance by vision alone is not sufficient. We need to use compliance control method based on contact force information to accomplish fine-grained operations. In the paper, firstly, a geometric model-based joint angle selection criterion for force parameter identification is proposed, which can improve the stability and accuracy of force sensor parameter identification. Secondly, due to the unstable and too small values of the collected torque information, and in order to omit the tedious force analysis, as well as the costly trial-and-error process, we divide the shaft-hole assembly problem into two parts. One is to combine the point cloud normal vector estimation and posture transformation to achieve the control of the end point position of the axis body constant, while adjusting the posture of the shaft body by speed control; and the other is to use the force feedback damping control to complete the assembly tasks when the shaft body direction is consistent with the hole axis direction. After these two parts of operation, the decoupling of posture and position can be realized, shaft hole assembly at any posture of the workpiece (hole) can be completed. The effectiveness and feasibility of the algorithm is verified by conducting experiments on the UR5 robot.**

Keywords—Parameter identification, Sample selection criterion, Posture adjustment, compliance control, force feedback damping control, shaft--hole assembly.

I. INTRODUCTION

Shaft-hole assembly is a widely discussed topic in the field of robotic assembly. There are three main approaches to achieve this task: one is to use the Remote Center Compliance device; the other is to use active compliance control algorithm; and the last is to use a learning algorithm, which has emerged in recent years. The scenario of shaft-hole is also divided into three cases: shaft-hole with chamfering, shaft-hole without chamfering (straight insertion), and special assembly.

It is a traditional and basic practice to obtain control rates from the analysis of different types of shaft-hole contact and force analysis. T. Tsuruoka, H. Fujioka et al. introduce the relationship between contact types and parameters of cylindrical pins and cylindrical holes with chamfers[1], M. Shahinpoor and H. Zohoor present the jack dynamics control equations for six different cases. Although the above methods can be mathematically analyzed to obtain exact solutions[2], they often require complex modeling analysis and calculations, and the existence of errors in the modeling itself can lead to limitations in the usefulness of such methods.

For this reason, many scholars have proposed various adaptive control methods, Some scholars have suggested that a method to achieve shaft-hole assembly by continuously exploring contact combined with a compliance control method[3], Some proposes a method that can adapt the force information during human demonstration by adjusting the Cartesian trajectory[4]. However, these methods are also unable to avoid the frequent collision process between hole and shaft. E. Mobedi et al. introduces the detection of assembly object pose by vision method and then applies it to plan the robotic arm trajectory[5], but the stiffness of the axis body will be greatly reduced due to the use of RCC equipment.

In response, this paper proposes a two-step control strategy that first uses point cloud normal vector estimation to estimate the hole axis direction, then controls the shaft posture by posture transformation, and then uses compliance control method for assembly task. Before this experiment, we have roughly moved the end of the shaft above the hole, but the posture and the exact position of the shaft are unknown, and by our method, we can accomplish the task of shaft-hole assembly with less collision in any posture of the hole.

Before performing the compliance control, it is first necessary to remove the gravity of the shaft, as well as the temperature drift and mounting force components from the data collected by the force sensor. For this purpose, a model needs to be constructed for parameter identification[6]. Considering the high cost of collecting recognition samples by robotic arm and the need to improve the recognition accuracy, we propose a geometric model-based sample selection criterion.

*Resrach supported by National Natural Science Foundation of China(52075531), Research on torso-arm cooperative compliance mechanism and control method considering flexo-rigid dynamics coupling.

Yong Jiang is with State Key Laboratory of Robotics, Shenyang Institute of Automation, Chinese Academy of Sciences, Shenyang 110016,China, Institutes for Robotics and Intelligent Manufacturing, Chinese Academy of Sciences, Shenyang 110169, China (corresponding author to provide phone: +86-024-23970277; e-mail: jiangyong@sia.cn).

Junhe Wang and Song Lin, are with State Key Laboratory of Robotics, Shenyang Institute of Automation, Chinese Academy of Sciences, Shenyang 110016, China, Institutes for Robotics and Intelligent Manufacturing, Chinese Academy of Sciences, Shenyang 110169, China, University of Chinese Academy of Sciences,Beijing100049,China(e-mail :1619356172@qq.com,linsong@sia.cn).

Fanxu Kong is with Shenyang Institute of Automation, Chinese Academy of Sciences, Shenyang 110016, China(e-mail:kongfanxu@sia.cn)

II. METHOD

Force parameter identification generally uses the least squares identification method, but since its samples come from the results of the actual control of the robotic arm, it takes more time and cost to collect more samples. Since there are many joint angles of the robotic arm, no specific selection criteria are given in the existing papers to enable us to reduce the number of samples while achieving efficient identification. Therefore, in this paper, we design a geometric model-based joint angle selection criterion for implementing six-dimensional force sensor parameter identification, taking the shaft-hole assembly task as an example.

In the control part, we use the point cloud to extract the workpiece normal vector (hole axis direction) and use it as the target posture of the shaft end coordinate system. Then we get the posture adjustment quantity in the shaft end coordinate system through posture transformation, and then convert it to the velocity adjustment quantity in the world coordinate system to realize the control of the shaft body direction in line with the hole axis direction. Finally, the assembly task is realized by force feedback damping control.

A. Joint angle selection criteria based on geometric model

First, since the samples for force sensor parameter identification need to be obtained through the actual control robotic arm, and the relationship between the joint angle of the robotic arm and the independent variables is many-to-one, As shown in Fig. 1. It becomes especially critical to design the sample selection criteria to achieve accurate parameter identification with a small number of samples.

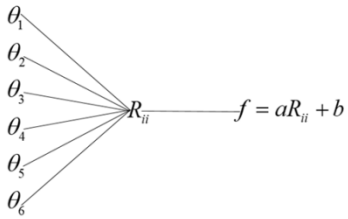

Figure 1. The joint angle corresponds to the independent variable

The UR5 robotic arm has six joint angles, and their different combinations make up the individual components of the arm's rotation matrix. The values of some of these components of the rotation matrix are used as independent variables in the parameter identification equation and participate in the parameter identification task.

Second, in this identification experiment, the independent variables of all the identification equations are the components of each axis of the end coordinate system in the z-axis of the base coordinate. Although they all come from the joint angles of the robotic arm, the independent variables are all different due to the number of joint angles that make up the independent variables and the way they are composed Since the identification needs to be carried out by means of parameter decoupling, it is necessary to design a batch of joint angle groups that can be repeatedly applied to all equations, taking into account the identification samples of each equation, so as to improve the efficiency of collecting samples while accurately completing the parameter identification.

For this purpose we propose the following guidelines for joint angle selection based on the geometric model.

I. The first three joint angle values are unchanged in all joint angle groups

The first three joint angle values are unchanged in all joint angle groups; the independent variables in the equation are all related to the rotation component, the first three joint angles of the robotic arm play a major role in the end position of the robotic arm, and the control of rotation is mainly concentrated in the last three joint angles, so the first three joint angles are fixed in order to ensure the safety of the parameter identification process. The experimental verification (See Fig. 2) proves that only the end three joints can still meet the requirements.

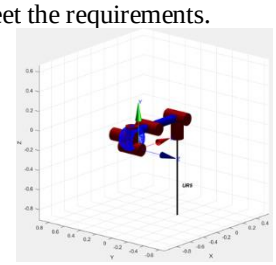

Figure 2. Working space of the robot when fixing the first three joints

II. Design samples for accurate identification based on the geometric information contained in the equations:

To reduce the number of samples required for identification, we need to consider a class of geometric shapes represented by the equations. The samples are set in terms of the minimum number of data points required to form this geometry. Suppose the geometry represented by the equation to be identified is a spatial plane, and we know that three points that are not collinear can uniquely determine a plane. Therefore, we set the independent variable of the sample to be identified by taking equally spaced points from the circle, so that the spatial plane in any direction can be accurately identified. As shown in Fig. 3.

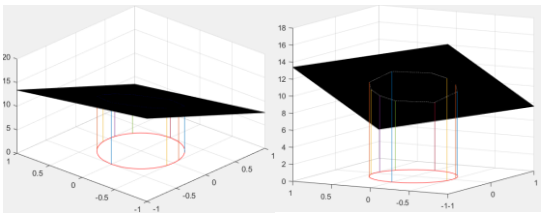

Figure 3. Independent variables for the identification of plane equations

III. Starting from the equation containing the least number of free joint angles, determine the values of each joint angle in turn:

After Ⅰ, We have fixed some of the joint angles, and the remaining joint angles are called free joint angles.

We aim to use the minimum number of free joint angles for identification to ensure that the next identification is more favorable to achieve the need for samples that are selected. In particular, when multiple e-

quation independent variables consist of the minimum number of free joint angles, we need to design joint a ngles starting from simple equations. A specific examp le is Fig. 4.

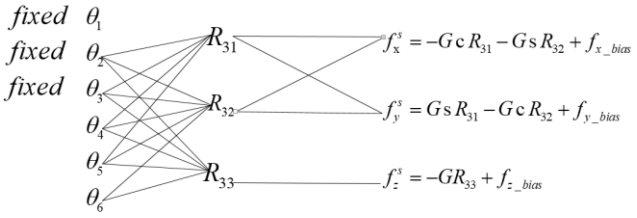

Figure 4. A specific example about criterion III

The relationship between the independent variables and the joint angles is shown in (3). After criterion I, the first equation contains the least number of free joint angles, and in order to use the least number of free joint angles for identification, we fix θ_4. uniformly sampled between $-pi/2$ and $pi/2$ as the value of θ_5. The value of the independent variable R_{33} is obtained as a straight line.For the remaining two equations, where the free joint angle is only θ_6. We let $\theta_6 = \theta_5$. Then the independent variables R_{31}, R_{32} take values in the interval of the circle with radius 0.5.

B. Posture adjustment with constant position

First, we estimate the point cloud normal vector using principal component analysis. In this project, the direction of the point cloud normal vector of the workpiece is exactly the direction of the hole axis. We use X to denote the point cloud scattering matrix, e to denote the direction vector, and u to denote the Lagrange multiplier function, for which we find the extrema and obtain the value of e as the eigenvector corresponding to the minimum eigenvalue of the scattering matrix, which is the normal vector to be estimated, i.e. the direction of the hole axis.

$$u = e^t Xe - \lambda(e^t e - 1)$$
$$Xe = \lambda e \quad (1)$$

The acquisition process is shown in Fig. 5.

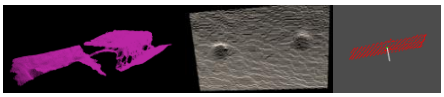

Figure 5. A specific example about criterion III

The left side is the actual obtained point cloud of the workpiece surface; the middle is the extracted point cloud of the upper surface; the right side is the normal vector obtained by PCA after down sampling.

We take this direction as the z-axis of the target coordinate system, and then get the rotation transformation matrix from the target coordinate system to the shaft end coordinate system, and the two coordinate systems are shown in Fig. 6.

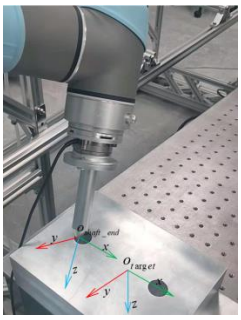

Figure 6. A pose transformation map

After obtaining the rotational transformation matrix, the rotational transformation matrix is converted into Euler angles rotating around the axis end coordinate system, then multiplied by the positive kinematic matrix T to obtain the angle Ω in the base coordinate system, then multiplied by the velocity coefficient vector C to obtain the desired velocity Vend in the base coordinate system, and finally multiplied by the inverse matrix of the Jacobi matrix to obtain the joint velocity Vq. The control block diagram is shown in Fig. 7.

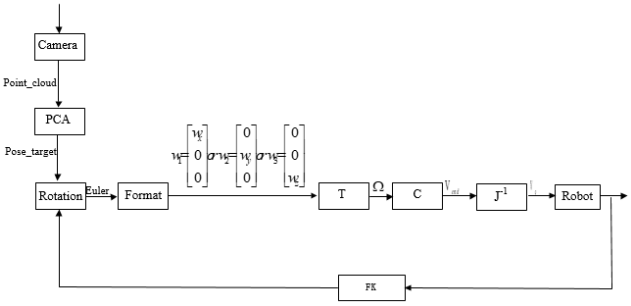

Figure 7. Posture control block diagram

C. Force feedback damping control

The control is based on the hybrid control framework of force and position. The position based control is carried out in the z-axis where the force information is not needed, and the force feedback control is carried out in the x-axis and y-axis where the force information is needed. The function selection matrix S is used to distinguish two parts of control.

In order to avoid the relatively long calculation time of inverse kinematics, and for the sake of safety, we use the speed based control method.

Since our expected goal is to insert the shaft into the hole, the z-axis will be set to a fixed speed value. In the X, Y axis control, we first get the contact force, then get the force in the base coordinate system by coordinate transformation, multiply it by damping matrix B to get the desired end velocity, and finally get the joint angular velocity by the inverse matrix of Jacobian matrix. The control block diagram is shown in Fig. 8.

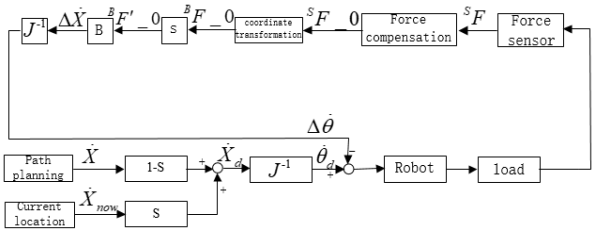

Figure 8. Block diagram of force feedback damping control

III. EXPERIMENT

The hardware environment for this experimental environment is a UR5 robot, RMA23820 six-dimensional force sensor of company ATI, and a D435i RGBD camera. The software environment includes Ubuntu 16.04 system, ROS robotics system, and software packages such as Camera SDK package and robot kinematics library KDL.

Since in this paper, the control of the robot is based on speed, in order to reduce the time delay of the control system and improve the response speed of the control, the socket method is used to communicate and send ur script language to the controller as a string to control the joint angular speed directly. In ROS system, on the other hand, communication is performed by writing topics, through the publish and subscribe mechanism, and adjusting the control frequency by changing the topic publish rate.

The actual operating system is divided into two parts, the parameter identification part and the shaft hole assembly part, and the parameter identification part needs to be performed before the experiment starts. The shaft hole assembly part can be further divided into two parts, which are the posture adjustment and the shaft hole assembly parts. In the program design, we use the rotation matrix between the target coordinate system and the current shaft end coordinate system of the robotic arm to determine which part of the control should be executed. In our experiment this is done by judging whether the element r_{33} of the rotation matrix is approximately equal to 1.

$$R=\begin{bmatrix} r_{11} & r_{12} & r_{13} \\ r_{21} & r_{22} & r_{23} \\ r_{31} & r_{32} & r_{33} \end{bmatrix} \tag{2}$$

A. *Model Building*

I. Robot kinematic model

The kinematic modeling of the robotic arm is the basis for analyzing robot-related problems. Firstly, the link pa are determined by the DH parameter method to model the robotic arm; then the coordinate transformation between the links is described by the link transformation matrix; finally, the homogeneous transformation matrix of the joint space to end Cartesian space mapping is obtained by concatenating the link transformation matrix. The DH parameter method consists of standard and modified forms, and here we choose to model the UR5 robotic arm using the standard DH parameter method, The DH parameter table and kinematic model are shown in Table I and Fig. 9, respectively.

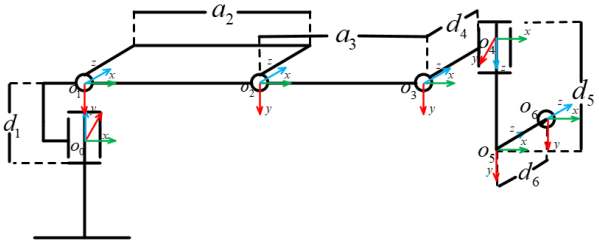

Figure 9. UR5 robotic arm kinematic model

TABLE I. DH PARAMETER

i	θ (rad)	α (rad)	a (m)	d (m)
1	θ_1	$-pi/2$	0	$d_1=0.0892$
2	θ_2	0	$a_2=-0.425$	0
3	θ_3	0	$a_3=-0.392$	0
4	θ_4	$-pi/2$	0	$d_4=0.1093$
5	θ_5	$pi/2$	0	$d_5=0.09475$
6	θ_6	0	0	$d_6=0.0825$

The components of each axis of the end coordinate system in the base coordinate z-axis are obtained as follows.

$$\begin{aligned} R_{31} &= \mathrm{s}(\theta_6)*\mathrm{c}(\theta_2+\theta_3+\theta_4)+\mathrm{c}(\theta_5)*\mathrm{c}(\theta_6)*\mathrm{s}(\theta_2+\theta_3+\theta_4) \\ R_{32} &= \mathrm{c}(\theta_6)*\mathrm{c}(\theta_2+\theta_3+\theta_4)-\mathrm{c}(\theta_5)*\mathrm{s}(\theta_6)*\mathrm{s}(\theta_2+\theta_3+\theta_4) \\ R_{33} &= -\mathrm{s}(\theta_5)*\mathrm{s}(\theta_2+\theta_3+\theta_4) \end{aligned} \tag{3}$$

II. Force parameter identification model

The six-dimensional force transducer measures the force applied in the x, y, and z directions, and the amount of torque applied in the x, y, and z axes, respectively. Before assembling the hole, We first make sure that the contact force data measured by the six-dimensional force sensor in six dimensions is zero. When the robotic arm is in free space, the information measured by the six-dimensional force sensor includes gravity, temperature drift, and the component of the mounting force, respectively. The bias terms due to the temperature drift and the mounting force are denoted by f_{x_bias}, f_{y_bias}, $f_{z\_bias}, m_{x\_bias}, m_{y\_bias}, m_{z\_bias}$, respectively. Let point denote the center of mass of the load in the sensor coordinate system, and let $F_G=[0,0,-G,0,0,0]$ denote the generalized force vector in the base coordinate system. φ indicates a fixed angle of rotation of the force sensor coordinate system o_{sensor} about the z-axis of the end coordinate system o_{end} of the robotic arm (c and s denote cos(φ) and sin(φ)), denote the generalized gravity vector in the sensor coordinate system, F and M denote the measured force and moment information. Fig. 10 shows the connection of each component and the force diagram.

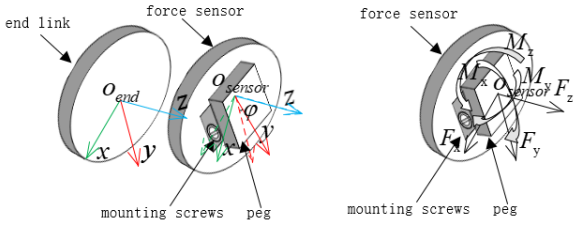

Figure 10. The connection of each component and the force diagram

The left side of the figure shows the fixed rotation angle between the force sensor coordinate system and the robotic arm end coordinate system, and the right side depicts the schematic diagram of the forces and moments in the sensor coordinates.

Thus we have the following equation.

$$F^s = \begin{bmatrix} f_x^s \\ f_y^s \\ f_z^s \\ m_x^s \\ m_y^s \\ m_z^s \end{bmatrix} = \begin{bmatrix} ({}^0R_6\ {}^6R_s)^{-1} & 0 \\ q\times({}^0R_6\ {}^6R_s)^{-1} & ({}^0R_6\ {}^6R_s)^{-1} \end{bmatrix} F_G + f\_bias \quad (4)$$

We take the above formula apart and get the following result.

$$f_x^s = -G\,c\,R_{31} - G\,s\,R_{32} + f_{x\_bias} \quad (5)$$

$$f_y^s = G\,s\,R_{31} - G\,c\,R_{32} + f_{y\_bias} \quad (6)$$

$$f_z^s = -GR_{33} + f_{z\_bias} \quad (7)$$

$$m_x^s = -G\,s\,q_z R_{31} + G\,c\,q_z R_{32} - Gq_y R_{33} + m_{x\_bias} \quad (8)$$

$$m_y^s = -G\,c\,q_z R_{31} - G\,s\,q_z R_{32} + Gq_x R_{33} + m_{y\_bias} \quad (9)$$

$$m_z^s = G\,c\,q_y R_{31} + G\,s\,q_y R_{32} + G\,s\,q_x R_{31} - G\,c\,q_x R_{32} + m_{z\_bias} \quad (10)$$

B. *Parameter identification experiments*

I. Sample Selection

Since we only need to consider the three-dimensional force information, only the first three equations need to be used in the identification. According to the criterion introduced earlier, the first three joint angles are fixed first, and then we start from the equation with the least free joint angle among the independent variables, see (7).

The formula for the independent variable R33 is given in (3). According to criterion I and III, we fix 1, 2, 3, 4 joints. According to criterion II, The geometry implied by this equation is a straight line, so we design the distribution of the independent variables to be uniformly distributed. We take equally spaced values in the approximate linear region of this $\sin(\theta)$ of $[-\frac{\pi}{2},\frac{\pi}{2}]$ as the value of θ_5. The final interval of the values of the independent variables is obtained as shown in Figure 11.

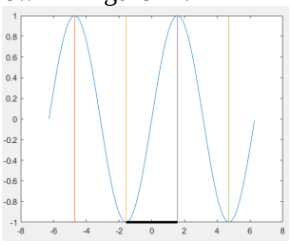

Figure 11. The range of values of the independent variable R33

The horizontal coordinate is the range of values of θ_5 and the vertical coordinate is the range of values of the independent variable R33.

From this equation we can obtain the value of G. Similarly, as mentioned in the previous example, the remaining equations represent the shapes of the two spatial planes. As mentioned in Fig. 7, we let $\theta_6=\theta_5$, and the following equation is obtained.

$$\begin{aligned} R_{31} &= \mathrm{c}(\theta_5)*\mathrm{c}(\theta_6) \\ R_{32} &= -\,\mathrm{c}(\theta_5)*\mathrm{s}(\theta_6) \end{aligned} \quad (11)$$

The values of the independent variables are obtained as shown in Fig. 12, respectively.

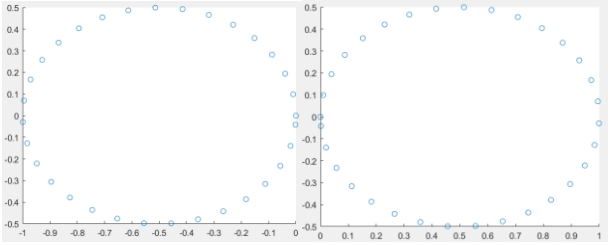

Figure 12. The range of values of independent variables R31 and R32.

The horizontal coordinate is the range of values of the independent variable R31 and the vertical coordinate is the range of values of the independent variable R32.

Finally, after writing the online parameter identification code on Linux, the identification errors were obtained as shown in the Table II. Compared with the existing parameter identification results, it is obvious that the stability and accuracy are improved.

TABLE II. PARAMETER IDENTIFICATION ERRORS

Identification error comparison		
Category	***Error mean (N/m)***	***Error maximum (N/m)***
Existing	fX:-0.288	fX:-0.674
	fY:0.1156	fY:0.9532
	fZ:0.9219	fZ:1.7203
Ours	fX:-0.261	fX:-0.3694
	fY:-0.153	fY:-0.3516
	fZ: -0.132	fZ:-0.2531

II. Parameter Adjustment

As the experiment progresses, the sensor temperature drift and the possible collision of the robotic arm will cause the final contact force information to deviate from that at the beginning. However, since the gravity value is accurately obtained after the identification is completed at the beginning, the only values that change are the temperature drift value and the loading force value. Therefore, in the actual experimental process, when an experiment is completed and the initial position is returned, we can update the bias value so that the identification error is the same as the error after the first identification.

C. *Shaft hole assembly experiment*

I. Posture adjustment

Posture adjustment is achieved by Euler angles, and in the specific control process, we do not wait for the

desired angle of rotation around one axis and then rotate around the other axes. Instead, The angular velocity of rotation around the x, y, and z axes of the shaft end coordinate system is assigned sequentially in each control cycle in the order of x-y-z Euler angles. This design allows for a shorter path for robotic arm posture adjustment and saves time and cost.

Figure 13. Posture adjustment experiment

II. Softening Jack

After the posture adjustment is achieved, the axis end coordinate system has been aligned with the target coordinate system. Since the sensor coordinate system is in the same posture as the shaft end coordinate system, and the force information value comes from the force sensor. Therefore, we control the velocity along the z-axis direction of the sensor coordinate system with a fixed downward velocity and set the value to 0.2m/s; in order to prevent the jitter caused by the identification error, we set the threshold value for the force feedback value of the compliance control, and the force value is sent to the control system as an input only when the absolute value of the force is greater than 1N/m.

The three-dimensional force curves are obtained as shown in Fig. 14.

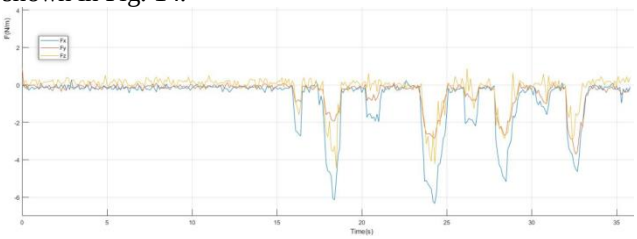

Figure 14. Block diagram of force feedback impedance control

IV. Conclusion

This paper is centered on two parts: parameter identification sample selection and shaft-hole assembly experiments. Firstly, a guideline that can be used to improve the sampling efficiency in the force sensor parameter identification process and can accomplish accurate parameter identification is introduced. Then a safe and stable method is proposed to reduce the collision during operation, which simplifies the complex assembly task into two parts: posture adjustment and compliance control. The experiments prove that all of the above methods are feasible and effective, which are of reference and guidance for related research in the field of robotics.

Appendix

Video Address
https://github.com/wangjunhe8127/Peg-Hole-assembly-in-real-world

References

[1] T. Tsuruoka, H. Fujioka, T. Moriyama and H. Mayeda, "3D analysis of contact in peg-hole insertion," Proceedings of the 1997 IEEE International Symposium on Assembly and Task Planning (ISATP'97) - Towards Flexible and Agile Assembly and Manufacturing -, Marina del Rey, CA, USA, 1997, pp. 84-89.

[2] M. Shahinpoor and H. Zohoor, "Analysis of dynamic insertion type assembly for manufacturing automation," Proceedings. 1991 IEEE International Conference on Robotics and Automation, Sacramento, CA, USA, 1991, pp. 2458-2464 vol.3.

[3] Hyeonjun Park, Ji-Hun Bae, Jae-Han Park, Moon-Hong Baeg and Jaeheung Park, "Intuitive peg-in-hole assembly strategy with a compliant manipulator," IEEE ISR 2013, Seoul, 2013, pp. 1-5.

[4] B. Nemec et al., "Transfer of assembly operations to new workpiece poses by adaptation to the desired force profile," 2013 16th International Conference on Advanced Robotics (ICAR), Montevideo, 2013, pp. 1-7.

[5] E. Mobedi, N. Villa, W. Kim and A. Ajoudani, "An Adaptive Control Approach to Robotic Assembly with Uncertainties in Vision and Dynamics," 2020 29th IEEE International Conference on Robot and Human Interactive Communication (RO-MAN), Naples, Italy, 2020, pp. 144-150.

[6] Binglong Wu, Daokui Qu, F. Xu, Jilai Song and Jintao Hu, "A multi-parameter overall identification method used for industrial robot force signal processing," Proceeding of the 11th World Congress on Intelligent Control and Automation, Shenyang, 2014, pp. 2437-2441.